JBR–BTR, 2014, 97: 233-238.

CAPILLARY TELANGIECTASIA OF THE BRAIN: IMAGING WITH VARIOUS MAGNETIC RESONANCE TECHNIQUES

F. Gelal, L. Karakaş, A. Sarsılmaz, K. Yücel, C. Dündar, M. Apaydın[1]

Brain capillary telangiectasia is an incidental vascular malformation found usually in pons and sometimes in extrapontine sites. Typical MRI features are enhancement on post contrast T1 weighted images and signal loss on gradient echo images. We evaluated 10 patients with various MR techniques. Susceptibility weighted imaging was superior to GRE T2 in showing decreased signal due to susceptibility effects. Diffusion weighted imaging and diffusion tensor imaging proved not useful in the diagnosis.

Key-word: Telangiectasia.

Capillary teleangiectasia of the brain (BCT) is a vascular malformation consisting of dilated capillaries separated by normal intervening brain parenchyma (1). They are usually discovered incidentally on contrast-enhanced magnetic resonance imaging (MRI) as an enhancing lesion. Finding out a contrast enhancing lesion in the brain arises concern about primary or metastatic brain tumors, demyelinating disease, inflammation or subacute ischemia (1, 2). BCT usually does not cause symptoms, although few patients with BCT having symptoms have been reported (1, 3, 4). Therefore, the differentiation of BCT from serious abnormalities that require treatment is essential to prevent unnecessary follow up or even invasive interventions.

BCT is usually invisible on computed tomography (CT) and occult on angiography (1). On MRI most of time the lesion is not visible on T1, T2 or FLAIR, although some hyperintensity can be seen on T2. On gradient-echo images BCT has been shown to be of low signal intensity (5-7). Low signal on T2*-weighted images has been attributed to susceptibility effects due to deoxyhemoglobin resulting from slow flow in the dilated vascular channels. Lately susceptibility weighted imaging (SWI) is being used in the diagnosis, since it has been shown to be more sensitive to susceptibility effects (2, 8-10). Diffusion weighted imaging (DWI) has also been used for the diagnosis of BCTs (1, 11, 12).

We aimed to further elucidate the imaging features of BCTs using various MRI sequences and techniques including gradient echo T2, SWI, DWI, Diffusion Tensor Imaging (DTI) and postcontrast imaging with spin echo T1 and 3D GRE T1.

Materials and methods

In this observational retrospective study, we screened the reports of 63.000 MRI examinations performed in our hospital from November 2009 until July 2012 using keywords in the hospital information system. We found 10 patients (6 female and 4 male patients; age range, 17-84 years; mean age 49 years, median age 57 years) having lesions consistent with capillary telangiectasia of the brain. Follow up examinations ranging from 4 months to 30 months (mean interval of 14 months) were available in 6 patients. Contrast enhancing lesions, located most of the time in pons, usually slightly hyperintense on T2 weighted images, which did not have mass effect and did not show any interval change in size or structure were diagnosed as capillary telangiectasia. Signal loss on gradient echo T2 and/or SWI further contributed to the diagnosis. MR images were evaluated by two radiologists in consensus. Any accompanying vascular abnormalities were noted.

MRI examinations were performed on a 1.5 Tesla scanner (GE Signa HDxt, General Electric Medical Systems, Milwaukee, WI) using 8 channel head coil. The protocol consisted of axial spin echo T2 and T1 weighted images, FLAIR T2 axial, postcontrast T1 weighted images in three orthogonal planes. Various gadolinium containing contrast agents were administered at a concentration of 0.1 mmol/kg for contrast enhanced imaging. Susceptibility weighted imaging was performed in 8 patients with the following scanning parameters: GRE EPI; TR/TE, 5750/25 ms; flip angle, 90 degrees; matrix, 256 x 512; FOV, 280 x 280 mm; slice thickness, 2.4 mm; spacing, 0 mm. Minimum intensity projection images were generated using the scanner's software. GRE T2 axial images were obtained in 6 patients with the parameters of: TR/TE, 840/24; flip angle, 25 degrees; matrix, 288x224; FOV, 240 x 180 mm; slice thickness, 5.5 mm; spacing, 2.0 mm. 1 mm^3 3D T1 GRE images (BRAVO) were obtained in 7 patients after contrast administration and the parameters were: TR/TE/TI, 12.3/5.2/420 ms; flip angle, 17 degrees; matrix, 288 x 288; FOV, 230 x 170 mm; slice thickness, 1.0 mm; spacing, 0 mm. DWI was performed in 7 patients with the parameters of: TR/TE, 6000/98.8; matrix, 148x128; FOV, 270 x 270 mm; slice thickness, 5.5 mm; spacing, 0.5 mm; b = 0 and b = 1000 values. ADC maps were generated by the scanner's software. DTI was performed in 6 patients using the following parameters: TR/TE; 6500/97.2; matrix, 128 x 128; FOV, 270 x 270 mm; slice thickness, 5.5 mm; spacing, 0 mm; 100 directions. Fractional anisotropy maps were generated offline and ROI measurements were performed from the lesion and symmetric normal parenchyma of pons. When the lesion was located at midline, ROI was placed midline at a lower slice where there was no lesion. ROI size was 83 mm^2 in lesions that were 10 mm or larger; and 39 mm^2 in lesions that were smaller. Two tailed student t test was used to compare ROI measurements from the lesion and normal parenchyma; $p < 0.05$ was considered statistically significant.

The reason for scanning was headache in 4 patients, seizure in 1 patient, anxiety disorder in 1 patient and carcinoma of breast, bladder and

From: 1. Department of Radiology, Izmir Katip Çelebi Üniversitesi Atatürk Eğitim ve Araştırma Hastanesi, Basın Sitesi, Izmir, Turkey.
Address for correspondence: Dr F. Gelal, M.D., Olimpiyat Köyü Atletizm Sok. 22/11, Balçova, Izmir 35330, Turkey. E-mail: fgelal@gmail.com

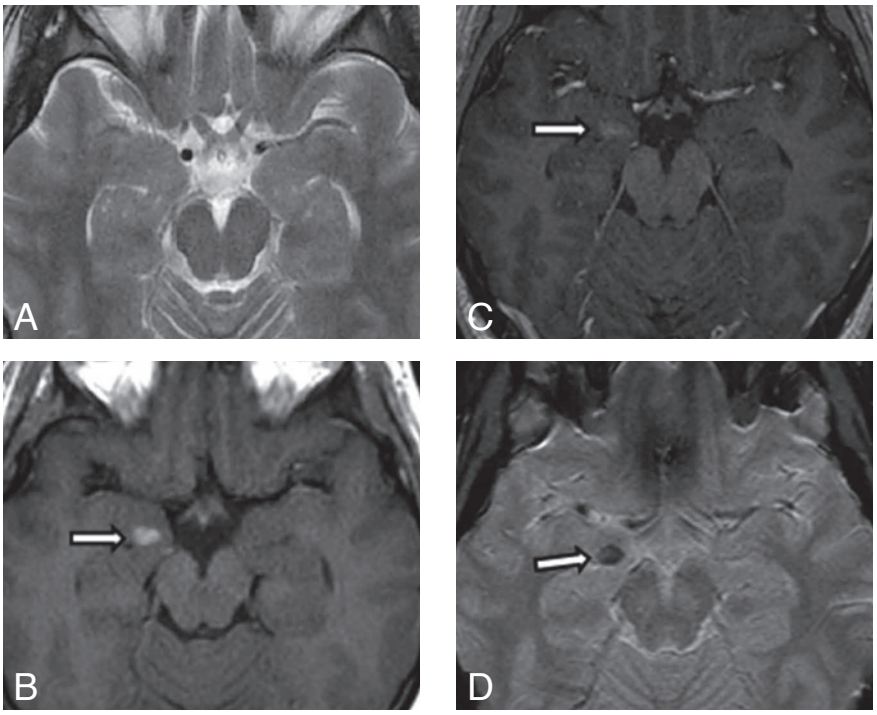

Fig. 1. — Capillary telangiectasia of the medial temporal lobe (Patient 6). A. SE T2 weighted image is normal. B. Postcontrast SE T1 weighted image shows a 7 mm enhancing medial temporal lobe lesion (arrow). It is isointense on T2, FLAIR and precontrast T1 weighted images. C. On postcontrast 3D GRE T1 enhancing lesion is less well seen (arrow). D. On SWI, the lesion shows marked signal loss (arrow).

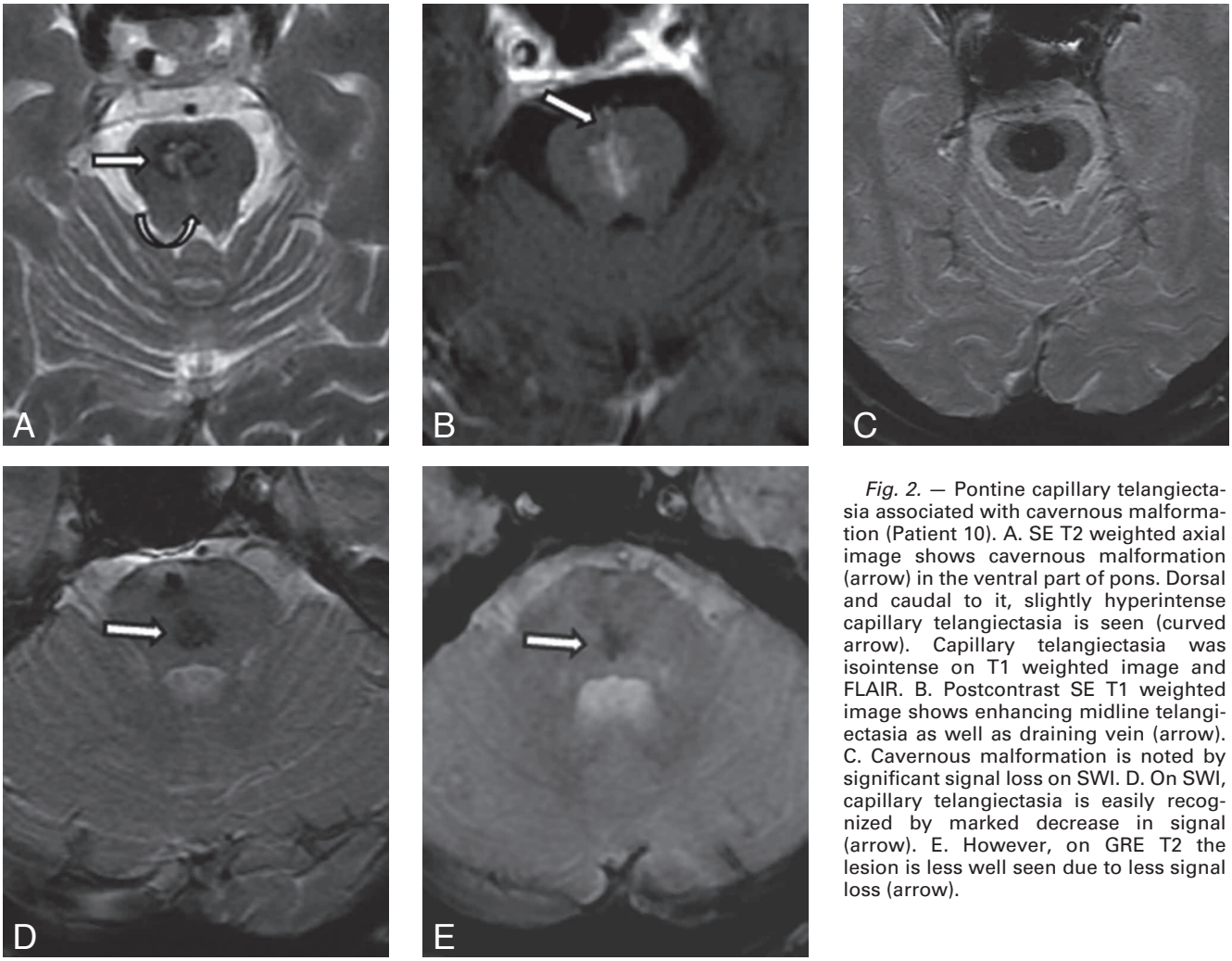

Fig. 2. — Pontine capillary telangiectasia associated with cavernous malformation (Patient 10). A. SE T2 weighted axial image shows cavernous malformation (arrow) in the ventral part of pons. Dorsal and caudal to it, slightly hyperintense capillary telangiectasia is seen (curved arrow). Capillary telangiectasia was isointense on T1 weighted image and FLAIR. B. Postcontrast SE T1 weighted image shows enhancing midline telangiectasia as well as draining vein (arrow). C. Cavernous malformation is noted by significant signal loss on SWI. D. On SWI, capillary telangiectasia is easily recognized by marked decrease in signal (arrow). E. However, on GRE T2 the lesion is less well seen due to less signal loss (arrow).

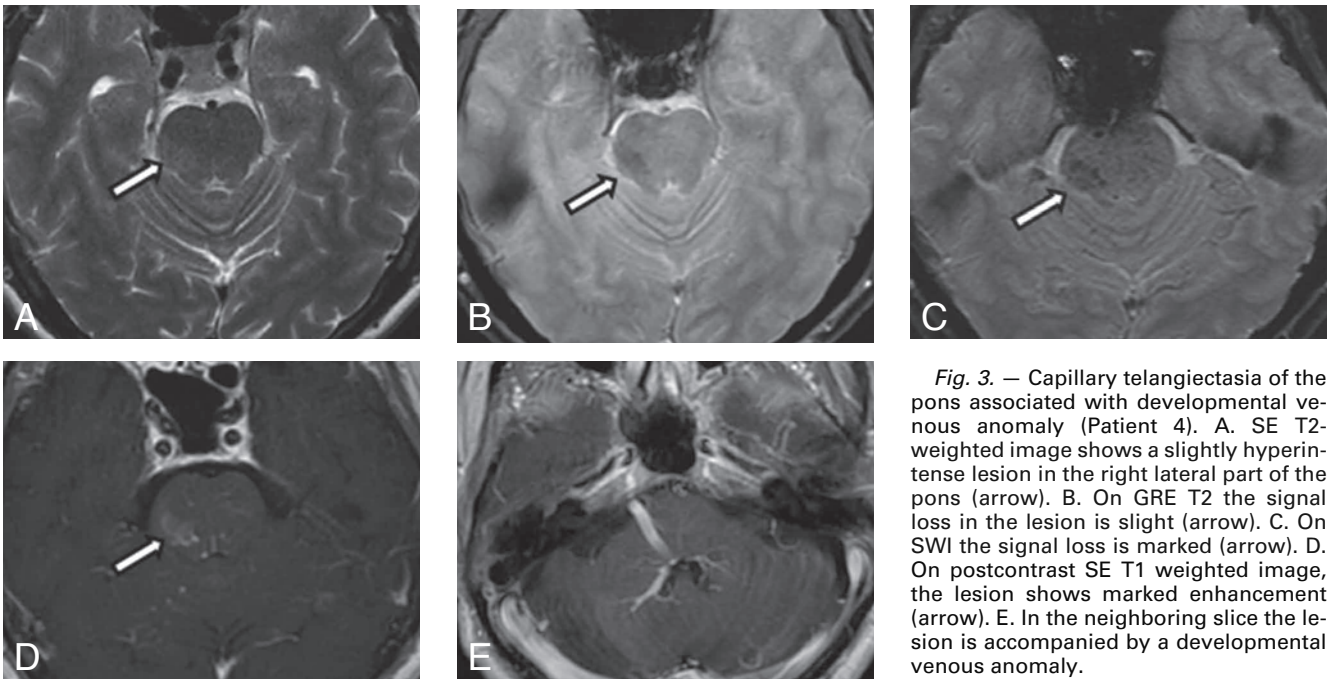

Fig. 3. — Capillary telangiectasia of the pons associated with developmental venous anomaly (Patient 4). A. SE T2-weighted image shows a slightly hyperintense lesion in the right lateral part of the pons (arrow). B. On GRE T2 the signal loss in the lesion is slight (arrow). C. On SWI the signal loss is marked (arrow). D. On postcontrast SE T1 weighted image, the lesion shows marked enhancement (arrow). E. In the neighboring slice the lesion is accompanied by a developmental venous anomaly.

lip in other 3 patients. None of the lesions in the patients with follow up, including those with primary malignancies, showed any interval change in size or structure over a mean follow up period of 14 months. In patient 6, a medial temporal lobe lesion was incidentally discovered during a pituitary MRI performed for hyperprolactinemia at an outside institution, and the lesion was presumed to be a tumor. All the lesions were incidental findings and irrelevant to patients' complaints.

Results

Nine lesions were located in pons (4 midline, 3 right parasagittal, 2 left parasagittal). One lesion was in the amygdala of the right medial temporal lobe (Fig. 1). The lesions ranged from 4 mm to 13 mm in size with a mean of 8.3 mm. One lesion was slightly hypointense on T1 weighted image, while all others were isointense. On T2 weighted images, 8 lesions were slightly hyperintense, 1 lesion was markedly hyperintense, while the temporal lobe lesion was isointense. On FLAIR T2 weighted images, 3 were slightly hyperintense and 7 were isointense (Table I).

On spin echo T1 weighted images contrast enhancement was marked in 7 lesions and slight in 3 lesions, whereas on 3D GRE T1 weighted images enhancement was slight in 6 lesions and no enhancement was shown in 1 lesion. In 7 patients, in whom both sequences were obtained, spin echo T1 was superior to 3D GRE T1 in demonstrating contrast enhancement. On the other hand, 3D GRE T1 was superior to spin echo T1 in showing the enhancing vessel converging to capillary telangiectasia in 3 of 5 lesions.

Signal loss on SWI was noted in all 8 patients who had this scan. In 5 lesions signal loss was marked and in 3 lesions it was slight. Out of 6 patients who had GRE T2 sequence, 3 showed slight, 1 showed marked signal loss while the other 2 did not show any decrease in signal. SWI was superior to GRE T2 in demonstrating the signal loss in capillary telangiectasia.

Out of 7 patients who had DWI,in 4 patients the lesions were isointense on both DWI and ADC. In the other 3 patients, lesions were isointense, slightly hyperintense and markedly hypointense on DWI and slightly hyperintense on ADC. Six patients had DTI. There was no statistically significant difference between the fractional anisotropy values of the lesions compared with normal parenchyma ($p = 0.07$), although a trend toward decreased anisotropy in the lesions was found (Table I).

One patient had multiple cavernous malformations (CM) both in the posterior fossa and supratentorial parenchyma accompanying pontine capillary telangiectasia. A CM in one patient (Fig. 2) and a developmental venous anomaly (DVA) in another patient (Fig. 3) were found to be located very close to pontine capillary telangiectasias. In one patient with pontine lesion, there was a remote DVA in subinsular region.

Discussion

Vascular malformations of the central nervous system have been classified into four types: arteriovenous malformations, cavernous malformations, developmental venous anomalies (venous angiomas) and capillary telangiectasias (13). BCTs consist of localized collections of multiple thin-walled vascular channels interspersed within normal brain parenchyma. They constitute 16% to 20% of all central nervous system vascular malformations at autopsy series and are the second most common vascular malformation after DVAs (1, 2, 14).

BCTs are most of the time asymptomatic and with the increased use of high resolution MR imaging, they are being more frequently discovered incidentally. In our series, all BCTs were incidental findings and were irrelevant to patients' complaints. There have been few reports of symptomatic BCTs causing seizures, blurred vision, cranial nerve dysfunction, progressive spastic paraparesis, sensorineural hearing loss and even death (1, 3, 4). Hemorrhage associated with BCTs is rare, and when it occurs, it is believed to be due to the associated vascular malformation and only rarely due to the capillary telangiectasia (7). Sayama et al. reported that lesions larger than 1 cm were more prone to cause symptoms (1). Two of the

Table I. — Location, size, and MRI features of brain capillary telangiectasias as well as accompanying vascular anomalies (CM: cavernous malformation; DVA: developmental venous anomaly).

Patient	Location	Size (mm)	T1	T2	FLAIR	Signal loss on GRE T2	Signal loss on SWI	Enhancement on SE T1	Enhancement on 3D GRE T1	Visibility of enhancing vessel on SE T1	Visibility of enhancing vessel on 3D GRE T1	DWI	ADC	Accompanying vascular anomaly	Fractional Anisotropy (First:Lesion, Second: Normal symmetric parenchyma)
1	Pons midline	10	iso	↑	↑	none	slight	marked	slight	low	high	iso	iso	none	0.312(0.12) 0.314(0.10)
2	Pons left parasagittal	13	↓	↑↑	↑	marked	marked	marked	slight	none	none	↓↓↓	↑	multiple CM	0.386(0.11) 0.411(0.09)
3	Pons midline	10	iso	↑	iso	none	slight	slight	none	high	high	iso	iso	DVA right subinsular	0.400(0.11) 0.432(0.13)
4	Pons right parasagittal	10	iso	↑	↑	slight	marked	marked	slight	low	high	↑	↑	DVA perilesional	0.428(0.07) 0.493(0.10)
5	Pons right parasagittal	7	iso	↑	iso	slight	marked	marked	slight	none	none	iso	iso	none	0.342(0.06) 0.480(0.06)
6	Right amygdala	7	iso	iso	iso	-	marked	marked	slight	none	none	iso	iso	none	
7	Pons midline	6	iso	↑	iso	-	-	slight	-	high	-	-	-	none	-
8	Pons left parasagittal	5	iso	↑	iso	-	-	slight	-	none	none	-	-	none	-
9	Pons right parasagittal	4	iso	↑	iso	-	slight	marked	-	none	none	-	-	none	-
10	Pons midline	11	iso	↑	iso	slight	marked	marked	slight	low	high	iso	↑	CM perilesional	0.401(0.05) 0.415(0.06)

patients in our study had lesions larger than 1 cm, although they were asymptomatic.

While pons is the most common location for BCTs, other locations have been reported. In one series, 8 of 33 lesions were located in frontal lobe, occipital white matter and basal ganglia (2). Supratentorial lesions arise more concern for malignancy than pons lesions, and these may even undergo surgical resection or biopsy (1, 7). The medial temporal lobe lesion in our series was presumed to be a tumor at an outside institution.

On T2, FLAIR or noncontrast T1 weighted images, some BCTs may go undetected. On precontrast images, we had only one lesion that was not detected, while 61% and 25% of BCTs were undetected in other series (2, 6). BCTs always enhance on postcontrast T1 weighted images. In some patients, as part of our higher resolution MR imaging protocol, we used 3D GRE T1 as well as SE T1 after contrast injection and showed that spin echo T1 was better than 3D GRE T1 in demonstrating contrast enhancement, while 3D GRE T1 was better than spin echo T1 in showing visibility of the enhancing vessel converging to BCT. This finding is compatible with literature findings (2) and can be explained by the fact that spin echo T1 has higher contrast resolution and lower spatial resolution than 3D GRE T1.

It is well known that BCTs demonstrate decreased signal on GRE images, probably owing to susceptibility effects of deoxyhemoglobin in the slow flow vascular channels. This finding has been found to be very helpful in the diagnosis (5, 6, 7, 12). Recently, susceptibility weighted imaging (SWI), known to be more sensitive to susceptibility effects than GRE imaging, has been used in the diagnosis of BCTs (2, 8, 9,10). SWI is a high spatial resolution 3D gradient echo MR technique which is very sensitive to intravascular venous (deoxygenated) blood as well as extravascular blood products (15). We found that SWI was more successful than GRE T2 in the diagnosis of BCTs. In our study, 2 lesions were isointense on GRE T2, while hypointense on SWI. Other authors have also reported several cases of BCTs, undetected by GRE T2 and shown to be hypointense on SWI (2, 10). However, the difference in the capabilities of the two techniques in detecting BCTs, may, in part, be due to thinner sections used in SWI compared to thicker slices used in GRE T2.

DWI has also been used in the diagnosis of BCTs. In a recent paper, it was reported that all 18 BCTs in pons showed decreased signal on DWI and this helped to differentiate BCT from tumor, inflammation or ischemia (11). On the contrary, other authors have shown that only 10% of 105 BCTs were hypointense on DWI (1). Our findings support the latter study. Four of the 7 lesions were isointense on both DWI and ADC; while the other 3 showed slightly increased signal on ADC. DTI characteristics of BCTs have not been reported before. We measured fractional anisotropy (FA) values of 6 lesions in comparison with normal parenchyma. Although there was no statistically significant difference in FA values, there was a trend toward decreased anisotropy, probably reflecting loss of normal white matter tracts. Small size of some lesions might have decreased the reliability of FA measurements. A DTI study comparing FA values of BCTs and other brain lesions might be helpful in determining whether or not this technique can be used to make a diagnosis in individual patients.

Capillary telangiectasia is considered to be an acquired lesion, rather than a primary developmental anomaly, and the frequent presence of an associated draining vein is believed to support this hypothesis (6). DVAs and CMs have been reported to coexist with capillary telangiectasias suggesting that venous restriction of capillary-venous outflow might have resulted in this vascular triad (16). These 3 malformations are also believed to exist on a continuum, so that a DVA may progress to a CM followed by the development of a capillary telangiectasia (17). Half of the lesions in our study had an associated drainage vein, while this was the case in 1/3 and 3/4 of lesions in two larger series (2, 6). A DVA in one patient and a CM in another were found adjacent to pontine capillary telangiectasias in our study, supporting the above assumption. None of the 6 patients with follow up, including the patient with perilesional DVA, showed any interval change in the size of the lesions or hemorrhage.

Absence of histopathological examination can be considered as a limitation of our study, but it is often not possible and necessary to obtain tissue diagnosis, since BCTs are benign and have fairly typical MR imaging features. Also since this was a retrospective study, it was not possible to use all of the above MR techniques in all patients. A prospective and larger study using all of these techniques in each patient may provide additional data.

In conclusion; BCT is an incidental vascular malformation found usually in pons and sometimes in extrapontine sites. It is hardly visible on precontrast MRI, while it enhances on postcontrast T1 weighted images and shows decreased signal on GRE T2 or SWI. These MRI findings are fairly typical for the diagnosis. Early and proper diagnosis using MRI avoids unnecessary follow up or surgical interventions. SWI is superior to GRE T2 in showing decreased signal due to susceptibility effects. DWI is not useful in the diagnosis contrary to what was reported in a previous publication. Further studies may be needed to clarify the role of DTI in the diagnosis. BCT is sometimes associated with other vascular malformations; in that case, follow up may be necessary to detect possible complications.

References

1. Sayama C.M., Osborn A.G., Chin S.S., Couldwell W.T.: Capillary telangiectasias: clinical,radiographic, and histopathological features. Clinical article. *J Neurosurg*, 2010, 113: 709-714
2. El-Koussy M., Schroth G., Gralla J., Brekenfeld C., Andres RH., Jung S., Shahin M.A., Lovblad KO., Kiefer C., Kottke R.: Susceptibility-weighted MR Imaging for diagnosis of capillary telangiectasia of the brain. *AJNR Am J Neuroradiol*, 2012, 33: 715-720. Epub 2011 Dec 22.
3. Huddle D.C., Chaloupka J.C., Sehgal V.: Clinically aggressive diffuse capillary telangiectasia of the brain stem: a clinical radiologic pathologic case study. *AJNR Am J Neuroradiol*, 1999, 20: 1674-1677.
4. Goyal M.K., Kumar G., Sahota P.K.: Reversible sensorineural hearing loss with normal brainstem auditory evoked potentials in pontine hemorrhage due to capillary telangiectasia. *J Clin Neurosci*, 2010, 17: 1198-1201. Epub 2010 Jun 8.
5. Lee R.R., Becher M.W., Benson M.L., Rigamonti D.: Brain capillarytelangiecasia: MR imaging appearance and clinicohistopathologic findings. *Radiology*, 1997, 205: 797-805.
6. Barr R.M., Dillon W.P., Wilson C.B.: Slow-flow vascular malformationsof the pons: capillary telangiectasias? *AJNR Am J Neuroradiol*, 1996, 17: 71-78.
7. Castillo M., Morrison T., Shaw J.A., Bouldin T.W.: MR imaging and histologic features of capillary telangiectasia of the basal ganglia. *AJNR Am J Neuroradiol*, 2001, 22: 1553-1555.
8. Sadana H.K.A.K., Lim T.A.: Large pontine capillary telangiectasia detected

by susceptibility-weighted imaging but inconspicuous on diffusion weighted imaging. *J HK Coll Radiol*, 2010, 12: 190-193.
9. Pendharkar H.S., Thomas B., Gupta A.K.: Susceptibility-weighted imaging in capillary telangiectasia. *Neurol India*, 2010, 58: 618-619.
10. Yoshida Y., Terae S., Kudo K., Tha K.K., Imamura M., Miyasaka K.: Capillary telangiectasia of the brain- stem diagnosed by susceptibility-weighted imaging. *J Comput Assist Tomogr*, 2006, 30: 980-982.
11. Finkenzeller T., Fellner F.A., Trenkler J., Schreyer A., Fellner C.: Capillary telangiectasias of the pons. Does diffusion-weighted MR increase diagnostic accuracy*? Eur J Radiol*, 2010, 74: e112-116.
12. Ozcan H.N., Avcu S., De Bleecker J., Lemmerling M.: MRI findings in giant pontine capillary telangiectasis associated with a developmental venous anomaly. *JBR-BTR*, 2011, 94: 293-294.
13. Dillon W.P.: Cryptic vascular malformations: controversies in terminology, diagnosis, pathophysiology, and treatment. *AJNR AmJ Neuroradiol*, 1997, 18: 1839-1846.
14. Chaloupka J.C., Huddle D.C.: Classification of vascular malformations of the central nervous system. *Neuroimaging Clin N Am* 1998, 8: 295-321.
15. Haacke E.M., Xu Y., Cheng Y.C., Reichenbach J.R.: Susceptibility-weighted imaging (SWI). *Magn Reson Med*, 2004, 52: 612.
16. Pozzati E., Marliani A.F., Zucchelli M., Foschini M.P., Dall'OlioM., Lanzino G.: The neurovascular triad: mixed cavernous, capillary,and venous malformations of the brainstem. *J Neurosurg*, 2007, 10: 1113-1119.
17. Abla A., Wait S.D., Uschold T., Lekovic G.P., Spetzler R.F.: Developmental venous anomaly, cavernous malformation and capillarytelangiectasia: spectrum of a single disease. *Acta Neurochir (Wien)*, 2008, 150: 487-489.